

# RSC Advances



This is an *Accepted Manuscript*, which has been through the Royal Society of Chemistry peer review process and has been accepted for publication.

*Accepted Manuscripts* are published online shortly after acceptance, before technical editing, formatting and proof reading. Using this free service, authors can make their results available to the community, in citable form, before we publish the edited article. This *Accepted Manuscript* will be replaced by the edited, formatted and paginated article as soon as this is available.

You can find more information about *Accepted Manuscripts* in the [Information for Authors](#).

Please note that technical editing may introduce minor changes to the text and/or graphics, which may alter content. The journal's standard [Terms & Conditions](#) and the [Ethical guidelines](#) still apply. In no event shall the Royal Society of Chemistry be held responsible for any errors or omissions in this *Accepted Manuscript* or any consequences arising from the use of any information it contains.

Fabrication and characterization of a novel nanofiltration membrane by the interfacial polymerization of 1,4-Diaminocyclohexane (DCH) and trimesoyl chloride (TMC)

Gui-E Chen<sup>a,\*</sup>, Yan-Jun Liu<sup>a</sup>, Zhen-Liang Xu<sup>b</sup>, Yong-Jian Tang<sup>b</sup>, Hui-Hong Huang<sup>a</sup>, Li Sun<sup>a</sup>

<sup>a</sup>*School of Chemical and Environmental Engineering, Shanghai Institute of Technology, 100 Haiquan Road, Shanghai 201418, China*

<sup>b</sup>*State Key Laboratory of Chemical Engineering, Membrane Science and Engineering R&D Lab, Chemical Engineering Research Center, East China University of Science and Technology, 130 Meilong Road, Shanghai 200237, China*

**ABSTRACTS:** This study focus on the preparation and nanofiltration properties of a novel thin-film composite polyamide membrane formed by the interfacial polymerization of 1,4-Diaminocyclohexane (DCH) and trimesoyl chloride(TMC) on a porous polysulfone supporting membrane. At the same time, we find that the introduction of Sodium N-cyclohexylsulfamate (SCHS) can improve a degree of the water flux and salt rejection. The active surface of the membrane was characterized by employing SEM and AFM. The performance of nanofiltration membrane was optimized by discussing the preparation condition, including monomer concentration, reaction time, curing condition and SCHS concentration. The result NF membrane prepared under the optimum condition exhibited Na<sub>2</sub>SO<sub>4</sub> rejection of 98.1% and the water flux of 44.6L·m<sup>-2</sup>·h<sup>-1</sup> under 0.6MPa. The pore size of the NF membrane is about 0.33-0.42nm which was calculated from the rejection of PEG and carbohydrates, respectively.

**Keywords:** Nanofiltration membrane interfacial polymerization Sodium N-cyclohexylsulfamate 1,4-Diaminocyclohexane

---

\* To whom all correspondence should be addressed.

Dr. Gui-E Chen, Email :chenguie@sit.edu.cn ; Tel : 86-21-64941192; Fax: 86-21-64941192.

## 1. Introduction

In the current progress of urbanization and industrialization in the world, the scarcity of potable water has become an alarming question, especially in arid region. To deal with water scarcity, many efforts have been made to remove heavy metals before its discharge and reuse wastewater. Nanofiltration (NF), as an important and environment-friendly separation technique between ultrafiltration and reverse osmosis, has attracted more and more research attention due to its low-energy consumption<sup>1</sup>, higher rejection of multivalent salts and molecular weight compounds (>300), and broad applications in the desalination of brackish water and seawater<sup>2</sup>, wastewater treatment<sup>3</sup>, and industrial substances separation<sup>4</sup>, etc. Therefore, nanofiltration membranes with good separation performance and other excellent property are required for more complicated applications.

At present, among the different successful NF membrane preparation techniques, interfacial polymerization is of particular interest because the selective layer and the porous support layer can be optimized separately<sup>5, 6</sup>. Though the number of applications for NF by interfacial polymerization increases steadily, this technology still suffers from some drawbacks, such as membrane fouling and insufficient separation factor<sup>7</sup>. Compared with membrane modification improvement, it is more accessible to ameliorate NF performance by finding out a novel monomer and adding to a outstanding additive. To address different separation requirements, a series of negatively charged nanofiltration membranes were prepared by exploiting new monomers or adding a new additive with special functional groups. These new monomers include polyhexamethylene guanidine hydrochloride<sup>8</sup>, tannic<sup>9</sup>, polyvinylamine<sup>10</sup>, N-aminoethyl piperazine propane sulfonate and PIP mixtures<sup>11</sup>, 2,2'-bis(1-hydroxyl-1-trifluoromethyl-2,2,2-trifluoroethyl)-4,4'-methylene-dianiline<sup>12</sup>, disulfonated bis[4-(3-aminophenoxy) phenyl] sulfone<sup>13</sup>, etc. Some additives are listed as follows: silica<sup>12</sup>, poly(styrene sulfonic acid) sodium salt<sup>14</sup>, TiO<sub>2</sub>, Al<sub>2</sub>O<sub>3</sub>, ZrO<sub>2</sub>, Al<sub>2</sub>O<sub>3</sub> and TiO<sub>2</sub> mixtures<sup>15</sup>, etc. Among all preparation methods, there is little report that aliphatic cyclic diamine as a monomer or amine salt as a additive.

In order to improve the nanofiltration membrane performance, such as salt rejection, water flux and antifouling performance, the information on the inherent material properties and surface structures of the active layer polymers are necessary. In this paper, we chose 1,4-

Diaminocyclohexane as water monomer to prepare a novel NF membrane, considering aliphatic amine has a ability of anti-fouling. Besides, Sodium N-cyclohexylsulfamate (SCHS) dissolved in aqueous phase was introduced as the additive during the interfacial polymerization process. The resulting NF membranes are measured by a cross-flow nanofiltration system (Fig.2), demonstrating their great potential. Remarkably, as an inorganic salt with negatively charge in solution, SCHS could not only improve the hydrophilicity and flux of the membrane, but also can enhance the anti-fouling of the membrane. In this work, different polymerization conditions on membrane performance were investigated, and the NF membrane performances were evaluated using different methods.



**Fig.1. Chemical structure of the monomers used: 1,4-Diaminocyclohexane (DCH) and trimesoyl chloride (TMC).**

## 2. Experimental

### 2.1 Materials

1,4-Diaminocyclohexane (DCH, purity>98%) was purchased Tansoole; Trimesoyl chloride(TMC, purity>98%) was bought from Qingdao Ocean Chemical Company. Their chemical structures are shown in Fig.1.

Polysulfone ultrafiltration (PSF-UF) supporting membranes (MWCO=70,000 Da) were fabricated in our lab. Sodium N-cyclohexylsulfamate (SCHS) was purchased from Tansoole; Other reagents were purchased from Sinopharm Chemical Reagent company which are of analytical grade purity without further purification.

### 2.2 Preparation of composite nanofiltration membranes

The composite NF membranes were fabricated by interfacial polymerization technique. PES ultrafiltration membranes were used as the porous support. PES ultrafiltration membranes were

washed thoroughly with water over 24h before using as porous support. Aqueous solutions of DCH and n-hexane solutions of TMC at different concentrations were prepared, respectively. PSF membranes were first soaked into aqueous solutions about 5min to ensure that DCH monomers can diffuse into porous support. The residual water on the surface was draining off by air knife. Second, the organic phase was poured on the top of the PSF UF membrane for a predetermined time (10-60s) for interfacial polymerization. The excess organic solution was removed from the surface, and the coated surfaces were air-dried in an oven at a certain temperature (post treatment temperature) for further polymerization reaction and hexane evaporation for a certain time (post treatment reaction time). Finally, the composite NF membranes were rinsed with deionized water and stored in 1% NaHSO<sub>3</sub> solution until it was tested.

### 2.3 Characterization of composite nanofiltration membranes

Membrane samples used for ATR-FTIR, SEM and AFM analysis were rinsed with de-ionized water for several times and dried under vacuum at 40°C for 24h.

The chemical structures of TFC membranes were characterized by FTIR-ATR (Perkin-Elmer Spectrum 2000 FTIR spectrometer) to confirm the existence of SCHS in the membrane and the interfacial polymerization reactions.

Scanning electron microscopy (SEM, S-3400N, Hitachi) was used to analysis the surface and cross-sectional morphologies of the composite NF membrane. Membranes were fractured in liquid nitrogen to obtain clean cut for cross sectional view. The samples were then gold sputtered for producing electrical conductivity.

Atomic force microscopy (AFM, Veeco, NanoScope III a Multimode AFM) was used to analyze the surface morphology and roughness of prepared membranes. The membrane surfaces were imaged in scan size of 5µm × 5µm. The surface roughness was reported in terms of root mean square (RMS).

Contact angle measurement instrument (JC2000D, PowerEach, China) was utilized to determine the water contact angle of NF membrane.

### 2.4 Permeability, rejection, pore size

Separation performance test of the resulting thin-film composite membranes were carried out at 0.6 MPa and 25.0°C employing a cross-flow nanofiltration system. The system (Fig.2) used for filtration contains membrane cell, plunger pump, pressure gauge and solution vessel. Membranes with an effective area of 75cm<sup>2</sup> were loaded into the cell for filtration. The feed for permeation test was de-ionized water or de-ionized water with added solutes such as Na<sub>2</sub>SO<sub>4</sub>, MgSO<sub>4</sub>, MgCl<sub>2</sub>, NaCl, or polyethylene glycol (PEG) of different molecular weights. The permeability was calculated by:

$$F = \frac{V}{A \times t}$$

Where  $V$  (L) is the total volume of the permeate collected under transmembrane pressure 0.6MPa on a time scale  $t$  (h) and  $A$  is the effective area of the membrane (m<sup>2</sup>). The solute rejection rate ( $R$ ) was calculated by:

$$R(\%) = 100 \times \left( 1 - \left( \frac{C_p}{C_f} \right) \right)$$

Where  $C_p$  and  $C_f$  are the solute concentration in permeate and feed solutions, respectively. The ion concentrations were measured by DDS-11A conductance meter (Shanghai Neici Instrument Company). According to the conductivity-concentration curves, the salts rejection rate was measured. The concentrations of organics were determined by TOC analyzer (TOC-VCPH, SHIMADZU, JAPAN). The results presented are average data with standard deviation from at least three samples of each type of membrane.

Pore size, pore size distribution and molecular weight cut-off (MWCO) of the SCHS /DCH-TMC NF membrane were calculated through two series permeation tests respectively, of which one test used a group of five PEG with molecular weights of 200, 400, 600, 1000, 2000Da as model solutes<sup>16</sup> and the other test used glucose, sucrose, raffinose as model solutes. Pore size distribution was calculated with the assumption of no gap and hydrodynamic interactions between the membrane material and the organic solutes. The MWCO value is taken by the molecular weight of the solute at the rejection by the membrane to 90%. The mean effective pore radius of the membrane ( $r_p$ ) is assumed the same with the geometric mean radius of the solute ( $r_s$ ) when  $R$  equals to 50%. The geometric standard deviation of the membrane ( $\sigma_p$ ) is assumed to be the

geometric standard deviation ( $\sigma_g$ ), which is the ratio of Stoke radius when R equals to 84.13 to that when R equals to 50%. Based on the hypothesis, the pore size distribution of membrane can be expressed as probability density function<sup>17-22</sup>

$$\frac{dR(r_p)}{dr_p} = \frac{1}{r_p \ln \sigma_p \sqrt{2\pi}} \exp \left[ -\frac{(\ln r_p - \ln u_p)^2}{2(\ln \sigma_p)^2} \right]$$

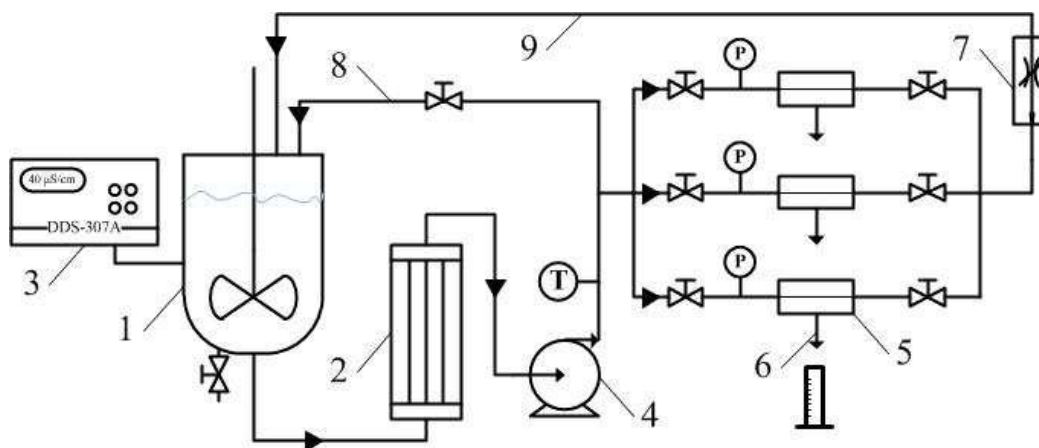
Where  $r_p$  is the Stokes radii of the organic solutes<sup>23</sup>.

The Stokes radii of the organic solutes used during the pore size distribution tests can be calculated from the following formulas<sup>18, 24</sup>:

$$\text{For PEG, } r_p = 16.73 \times 10^{-12} \times M^{0.557}$$

$$\text{For small molecules, } \ln r_p = -1.4962 + 0.4654 \ln M$$

Where  $M$  is the MW of the organic solutes.



1-Solution vessel, 2-Heat exchanger, 3- conductance meter, 4-Plunger pump, 5-Crossflow cell filled with membrane, 6-Permeate, 7-Flowmeter, 8- Bypass, 9- Concentrate valve.

**Fig.2.** Assessment equipment of nanofiltration

## 2.5 Anti-biofouling performance assessment of composite nanofiltration membranes

In the antifouling experiment, BSA was chosen as representative of protein in nature water source to evaluate the antifouling property of the NF membrane. A 500 mg/L BSA was forced to permeate through the membrane under an operation pressure of 0.6MPa, and the flux was recorded as  $J_w$ . The antifouling experiment was carried out over time of 24h. To analyze the antifouling properties in details, several ratios were defined<sup>11, 25-27</sup>. The flux decay ratio (DR) was calculated as follows:

$$DR = \left( \frac{J_{w0} - J_{wt}}{J_{w0}} \right) \times 100\%$$

Where  $J_{w0}$  and  $J_{wt}$  are fluxes at the initial and t time of antifouling test, respectively. The lower DR value means the better antifouling property of the nanofiltration membrane corresponding to slight deposition or adsorption of fouling on the membrane surface. After flux decay measurements, the solutions were then poured out and water was added in the filtration cell. The used nanofiltration membranes were cleaned directly in the cell for 30min under magnetic stirring. At last, the cell was emptied and refilled with water again. The water flux ( $J_{w2}$ ) of the cleaned membrane was measured. The flux recovery ratio ( $FRR$ ) was calculated as follows:

$$FRR = \left( \frac{J_{w2}}{J_{w0}} \right) \times 100\%$$

The higher  $FRR$  value, The better antifouling property of the nanofiltration membrane.

## 2.6 Long-term stability test of composite nanofiltration membranes

A long-term test was conducted at a pressure of 0.6MPa with 2000ppm  $\text{Na}_2\text{SO}_4$  aqueous solution at PH 7.0 and 25.0°C to investigate the durability and performance stability of the result NF membrane. Periodical measurements were carried out to check the water flux and salt rejection of the membrane.

## 3. Results and discussion

### 3.1 Chemical structures of membrane surface

FTIR spectrum of DCH and SCHS sample, ATR-FTIR spectra of PSF support membrane, DCH-TMC composite membrane and SCHS /DCH-TMC composite membrane are presented in Fig.3 to analyze the chemical structural changes of the composite membrane. Beside the typical PSF bands of the substrate, DCH-TMC composite membrane and SCHS /DCH-TMC composite membrane possessed additional peak at  $1651\text{cm}^{-1}$ (C=O stretch),  $1619\text{cm}^{-1}$ (N-H stretch) and  $1434\text{cm}^{-1}$ (C-N stretch) that corrected to amide group<sup>28-30</sup>. It can be seen from the figure that the interfacial polymerization among DCH and TMC had occurred out and a polyamide active layer was formed. Moreover, compared with DCH-TMC composite membrane, SCHS /DCH-TMC

composite membrane exhibited new peaks at 1111 and 951 $\text{cm}^{-1}$ , which are the characteristic absorbance of the S=O and S-N bond of sulfonamide group<sup>31</sup>. Based on the results of ATR-FTIR analysis, the chemical structure of the active skin layer formed through the reaction of TMC with DCH and SCHS is schematically shown in Fig.4, which also gives the formula for the polymerization step.

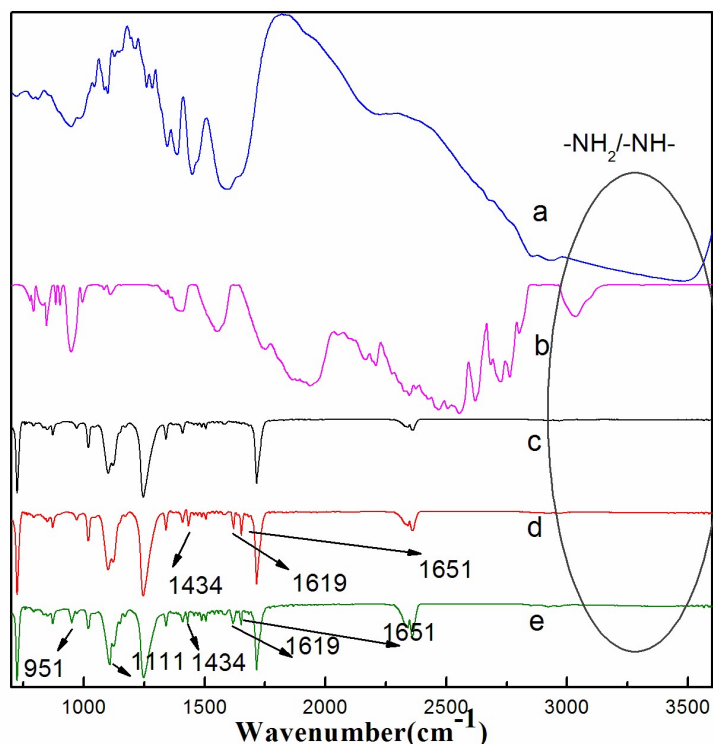


**Fig.3.** FTIR spectrum of (a) DCH and (b) SCHS, ATR-FTIR spectra of (c) PSF support membrane; (d) DCH-TMC composite membrane and (e) SCHS /DCH-TMC composite membrane.

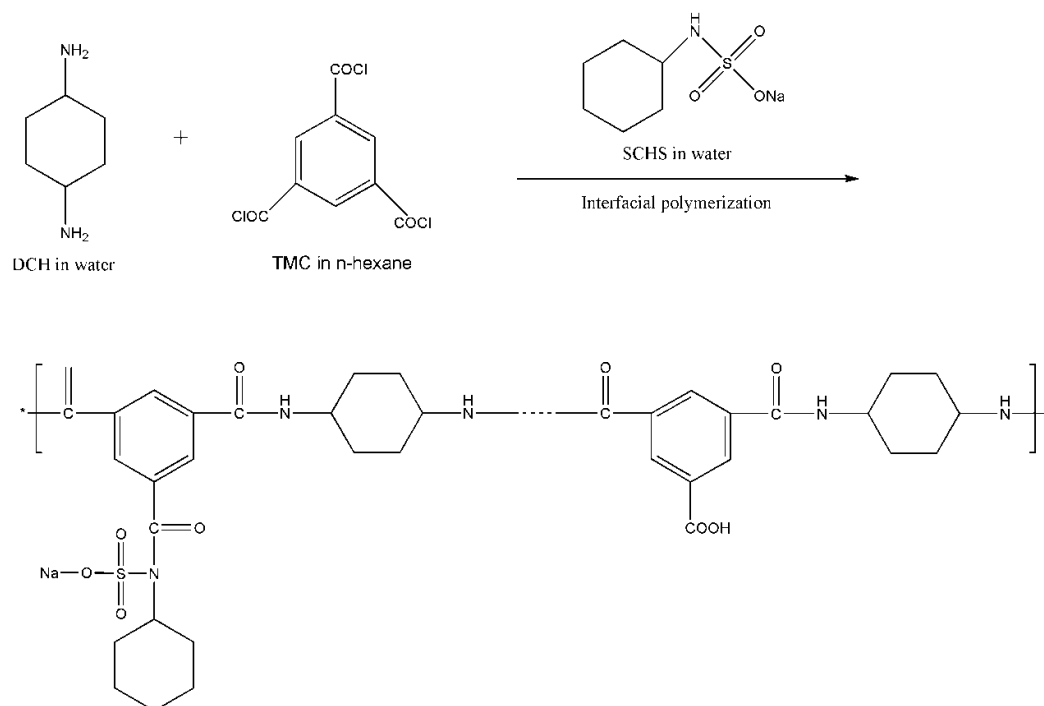


**Fig.4. Structure of polyamide skin layer formed by interfacial polymerization of CHD with TMC and SCHS**

### 3.2 Analysis of membrane morphology

The structure and surface roughness of the membrane were characterized by using SEM and AFM, respectively. The surface and cross-section morphology of membranes were visualized by SEM. It can be seen clearly that DCH-TMC composite membrane takes on a composite structure, namely a thin and dense active function layer existing on the porous polysulfone supporting membrane, and that adding SCHS results in an increase in skin layer density of the resulting membrane. After further measurement, the dense layer thickness of is about 200 nm. Quantitative analysis of the roughness of the surface area was made possible by image statistics in AFM. Average roughness (RMS) is defined as the mean of the root for the deviation from the standard surface<sup>23</sup>. In Fig.6, the RMS of various membrane are as follows: polysulfone support membrane is 5.57nm, DCH-TMC composite membrane is 227.34nm, SCHS /DCH-TMC composite membrane is 128.37nm, which is in good agreement with the SEM results.

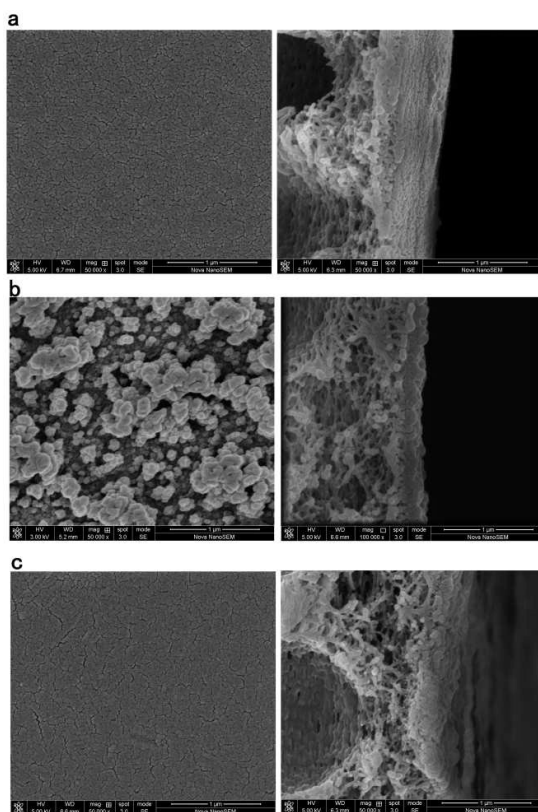


**Fig.5.** SEM images of the membrane (left: surface; right: cross section)(a) polysulfone support membrane, (b) DCH-TMC composite membrane, (c) SCHS /DCH-TMC composite membrane.

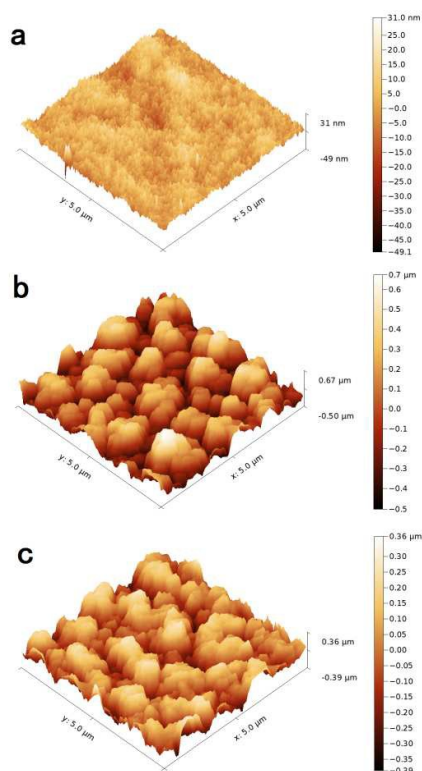


**Fig.6.** AFM images of surface morphologies of (a) polysulfone support membrane, (b) DCH-TMC composite membrane and (c) SCHS /DCH-TMC composite membrane

### 3.3 Effects of preparation conditions on filtration performance of the nanofiltration membranes

It's well-known that the performance of the composite nanofiltration membranes is determined by the chemistry and the preparation conditions of the thin selective layer<sup>32-38</sup>. In this section, NF performance of DCH-TMC/PSF composite membranes prepared with variable conditions was investigated to determine the optimized fabrication parameters.

#### 3.3.1 Monomers concentration

Influence of DCH concentration on filtration performance of nanofiltration membranes was first investigated and presented in Fig.7. The DCH-TMC NF membranes were prepared using different concentrations of DCH under the conditions of TMC concentration = 0.15%(w/v), reaction time = 15s, curing temperature =80°C and curing time = 5min.

It can be seen clearly from the figure that, when the DCH concentration aqueous phase was increased from 1.0 to 2.0% (w/v) at a fixed TMC concentration of 0.15% (w/v), the salt rejection of the membranes kept on increasing, while the water flux was decreased. When the DCH concentration exceeded 2.0% (w/v), the salt rejection changed slightly.

Similarly, the effect of the concentration of the TMC in organic phase was also investigated to optimize the performance of the DCH-TMC NF membrane. Fig.8 shows the performance of the composite membranes prepared under conditions of DCH concentration = 2.0% (w/v), reaction time = 15s, curing temperature =80°C and curing time = 5min. The salt rejection of the membranes increased at first until the TMC concentration in organic phase reached 0.25% (w/v), and then changed slightly while the water flux of the membranes decreased rapidly with the increasing TMC concentration to 0.50% (w/v).

This observation can be explained following the work of Freger on PA film formation kinetics and Nadler and Srebnik<sup>5,39-42</sup>. The concentrations of monomers in both the aqueous and organic phases have great effects on the rate of the interfacial polymerization. The interfacial polymerization occurring between a diamine and an acid chloride take place on the organic side of two phase interface. When DCH and/or TMC are at low concentration, the rate of reactions is expected to be lower and the polyamide skin layer is formed by low molecular weight polymer, which caused the lower salt rejection and higher water flux. With increase in DCH concentration and/or TMC concentration, the formation of thin barrier layer tends to be the maximum thickness and density since the film thickness remains almost unchanged. So the water flux is decreased and the salt rejection is increased. Further increase in the concentration of DCH and/or TMC, however, tends to have little effect on the rate and extent of polymerization. So the water flux and salt rejection change slightly.

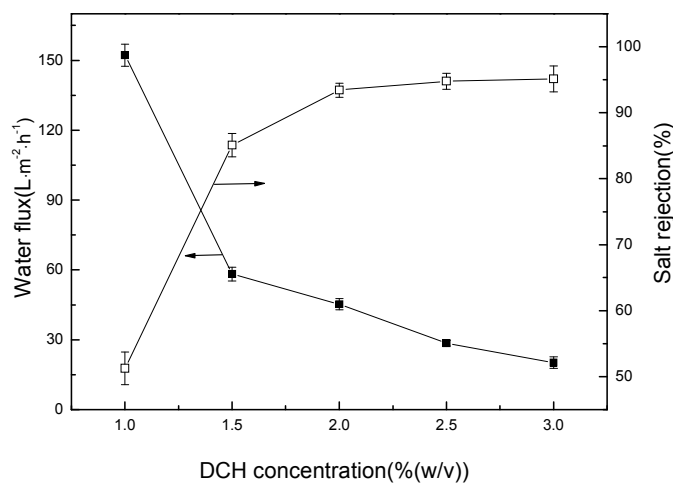


**Fig.7.** Effect of DCH concentration on salt rejection and water flux of the resulting membrane tested with 2000ppm Na<sub>2</sub>SO<sub>4</sub> aqueous solution at 0.6MPa, 25°C and PH 7.0.

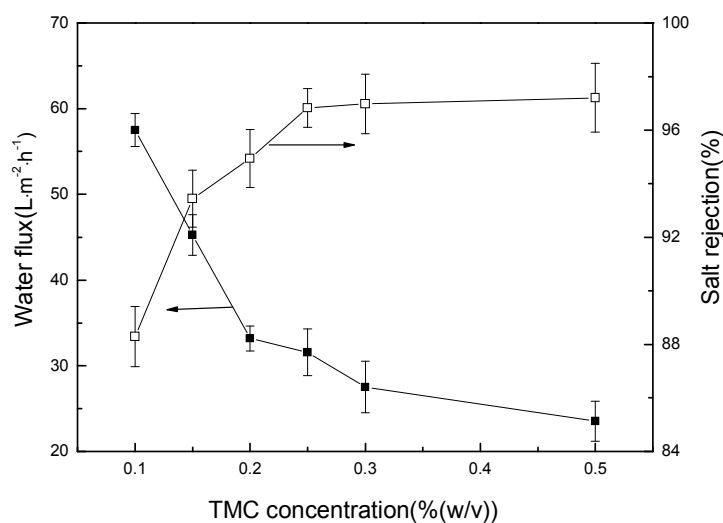


**Fig.8.** Effect of TMC concentration on salt rejection and water flux of the resulting membrane tested with 2000ppm Na<sub>2</sub>SO<sub>4</sub> aqueous solution at 0.6MPa, 25°C and PH 7.0.

### 3.3.2 Reaction time

The effect of the reaction time on membrane performance is shown in Fig.9. The membrane flux decreased quickly from 10 to 20s, and then decreased slightly from 20 to 60s. However, the membrane rejection increased quickly as the reaction time increased from 10 to 15s, and the increased slightly from 15 to 60s.

It's well known that the interfacial polymerization between DCH and TMC occurs on the organic side of the aqueous-organic interface, and the reaction is diffusion-controlled and exists in a self-limiting phenomenon. The reaction time plays an important role in determining the extent of polymerization, and thereby the cross-linking degree and thickness of top skin layer as well as the resulting membrane performance<sup>12, 42-45</sup>. The thickness of the active layer of the NF membrane increases with increasing reaction time. When the thickness of the active layer is enough to prevent DCH diffusing from aqueous phase into the organic phase, the top skin layer thickness will stop growing. So the density of the active layer had no significant change as the prolonged of reaction time from 20 to 60s. In this study, short reaction time lead to higher permeation of the water flux. As the reaction time increased, the water flux decreased and the salt rejection increased. Considering both good salt rejection and high water flux, the reaction time 15s was selected as the optimism reaction time to prepare the membranes.

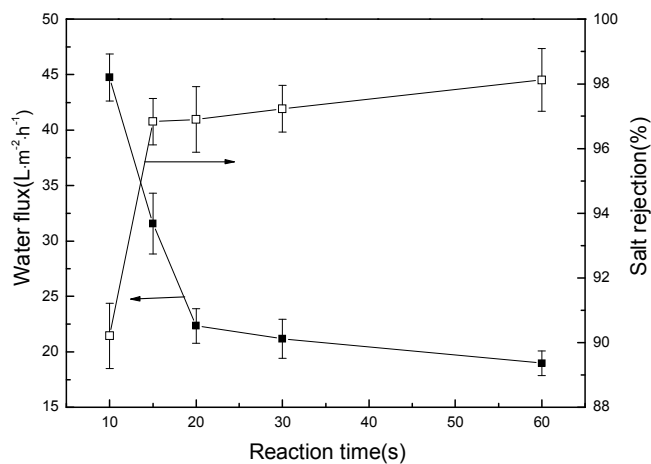


**Fig.9. Effect of interfacial reaction time on salt rejection and water flux of the resulting membrane tested with 2000ppm Na<sub>2</sub>SO<sub>4</sub> aqueous solution at 0.6MPa, 25°C and PH 7.0.**

### 3.3.3 Curing temperature and time

The treatment to the nascent polyamide composite membrane was helpful to the diffusion of the monomers into the interface for polymerization, which increased the cross-linking degree of the polymer film. The denser cross-linking structures led to a decreasing mass transport across membrane and a better mechanical property of the NF membrane<sup>5, 46</sup>. Table 1 shows that with the

increasing curing temperature from 40 to 80°C, two processes took place simultaneously: pore size kept decreasing appreciably and densification of the ultra-thin layer increased gradually which resulted in higher rejection with a marginal decreased in water flux. However, further increased in curing temperature or time resulted in the pore shrinkage of the support membranes and a much more compact structure of the skin layer with the consequent decrease in water flux<sup>46</sup>, which led to an overall decline in salt rejection. Considering the Na<sub>2</sub>SO<sub>4</sub> rejection and water flux together, the optimal curing time is for 5min at 80°C.

**Table 1 Effect of curing conditions on the performance of DCH-TMC NF membrane.**

Curing temperature <sup>a</sup> (°C)	Curing time <sup>a</sup> (min)	Na <sub>2</sub> SO <sub>4</sub> rejection <sup>b</sup> (%)	Water flux <sup>b</sup> (L/m <sup>2</sup> h)
40	5	75.62±1.21	47.08±1.23
60	5	80.78±1.34	44.57±2.78
80	3	90.73±0.89	37.81±1.97
80	5	96.83±0.72	31.56±2.73
80	10	97.31±1.01	23.43±1.99
100	5	85.39±2.01	28.56±2.33

<sup>a</sup> The membrane preparation condition: DCH concentration=2.0% (w/v), TMC concentration = 0.25% (w/v), reaction time =15s.

<sup>b</sup> Test conditions: feed= 2000ppm Na<sub>2</sub>SO<sub>4</sub> aqueous solution, pressure=0.6MPa, temperature=25.0°C and pH=7.0.

### 3.3.4 Sodium N-cyclohexylsulfamate(SCHS) concentration

The SCHS concentrations of composite NF membranes from 0 to 1.0% (w/v) were investigated under the following membrane preparation: 2% (w/v) DCH and a certain concentration of SCHS in the aqueous phase; 0.25 (w/v) TMC in the organic phase; reaction time for 15s and curing temperature at 80°C for 5min. Fig.10 shows the effect of SCHS concentration on salt rejection and water flux. With the SCHS concentration increased from 0 to 0.07% (w/v), the salt rejection increased from 96.8 to 98.1% (w/v) and the water flux increased from 31.6 to 44.6 m<sup>2</sup>h<sup>-1</sup>. When the SCHS concentration was further increased from 0.07 to 1% (w/v), the salt rejection decreased whereas water flux increased. It could be concluded that the proper SCHS concentration should be controlled near 0.07%. This phenomenon can be explained as follows: The rejection rate of the charged nanofiltration membrane to salt is mainly determined by both the size and Donnan exclusion effects<sup>47</sup>. With the increasing SCHS concentration, both the negative surface charge and pore size of the formed composite membrane increased, and the increased pore size would weaken the size exclusion effect, while the increased surface charge would enhance the

Donnan exclusion effect between the membrane surface and the anions. For salt  $\text{Na}_2\text{SO}_4$ , the enhancement of Donnan exclusion effect was dominant for the composite NF membrane prepared under the SCHS concentrations lower than 0.07% (w/v). Such phenomenon fit well with the result of rejection to different inorganic salts for NF composite membranes as Fig.11. As a result, the incorporation of SCHS led to the formation of composite NF membrane with improved  $\text{Na}_2\text{SO}_4$  rejection. However, the reverse was true for the composite NF membranes prepared with the SCHS concentrations higher than 0.07% (w/v), under which the weakening of size exclusion effect would be dominant, resulting in a decline of decline of rejection to  $\text{Na}_2\text{SO}_4$ .

Furthermore, when comparing the result composite membrane with other nanofiltration membrane which were described by other references like membrane PAMAM/PAN<sup>48</sup> ( $15.3 \text{ m}^2\text{h}^{-1}$ ,  $\text{Na}_2\text{SO}_4$  rejection 86.7%) and membrane MPD<sup>49</sup> (water flux:  $22.8 \text{ m}^2\text{h}^{-1}$ ,  $\text{Na}_2\text{SO}_4$  rejection 95.5%), the result composite membrane (water flux:  $44.6 \text{ m}^2\text{h}^{-1}$ , salt rejection 98.1%) has higher water flux or  $\text{Na}_2\text{SO}_4$  rejection.

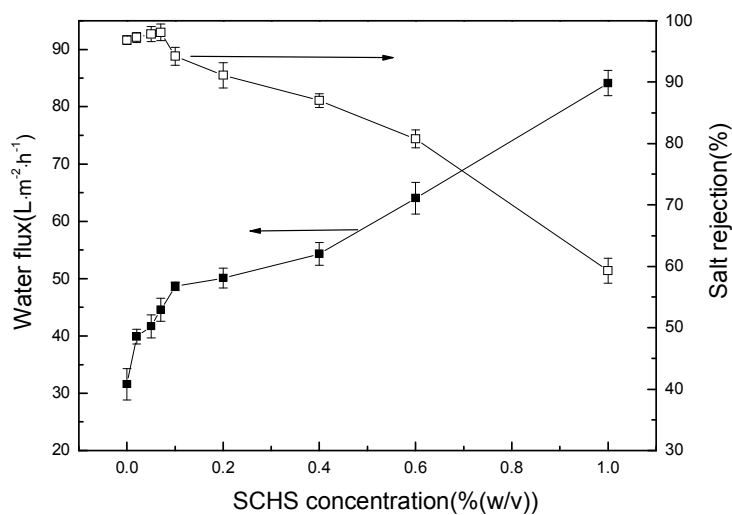


**Fig.10.** Effect of SCHS concentration on salt rejection and water flux of the resulting membrane tested with 2000ppm  $\text{Na}_2\text{SO}_4$  aqueous solution at 0.6MPa, 25°C and PH 7.0.

### 3.4 Separation performances of the optimized composite nanofiltration membrane

In this section, DCH-TMC/PSF NF membranes prepared with the optimized conditions were investigated to evaluate its potential application. The optimum condition is as follows: 2.0% (w/v)

DCH and 0.07% (w/v) SCHS in the aqueous phase; 0.25% (w/v) TMC in the organic phase; reaction time for 15s and curing temperature at 80 °C for 5min.

### 3.4.1 Inorganic salts and PEG rejection

The rejection rate of different inorganic salts was compared for membranes prepared from DCH-TMC and SCHS /DCH-TMC as shown in Fig.11. Four kinds of salt solution were used in the experiment. It was seen that the salt rejection of DCH-TMC or SCHS /DCH-TMC composite NF membrane decreased in the following order:  $\text{Na}_2\text{SO}_4 > \text{MgSO}_4 > \text{MgCl}_2 > \text{NaCl}$ , which demonstrated that the composite NF membranes were negatively charged membranes. In addition, the salt rejection of SCHS /DCH-TMC composite NF membrane was higher than DCH-TMC composite NF membrane's, which was more obviously for bivalent salts. The improvement in salt rejection was arising from the introduction of strong negatively charged function group on the active layer of SCHS /DCH-TMC composite NF membrane<sup>50,51</sup>.

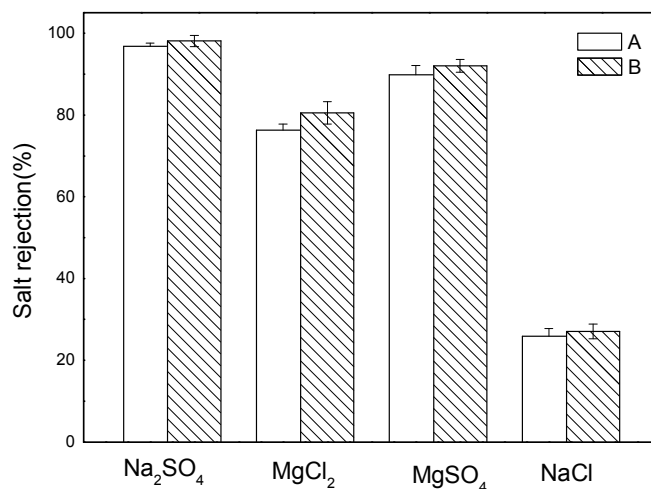


**Fig.11. Rejection of different inorganic salts for (A) DCH-TMC composite membrane and (B) SCHS /DCH-TMC NF membrane.**

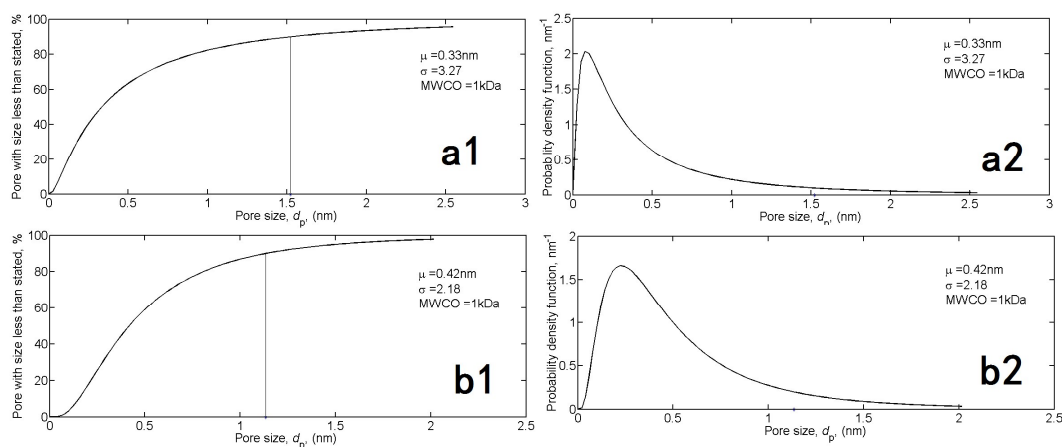
### 3.4.2 Pore size, pore size distribution and molecular weight cut-off (MWCO)

Table 2 shows the rejection of neutral solutes used during pore size distribution. Based on this, the pore size, pore size distribution and molecular weight cut-off (MWCO) of the SCHS /DCH-TMC NF membrane were calculated and showed in Fig.12. The probability density

function curves of the pore size distribution calculated on the rejections of PEG and carbohydrates were indicated in Fig.12 (a1) and Fig.12 (b1) respectively. It can be found that about 90% of the pore size is less than 1.5nm. The pore size obtained from the rejections of PEG and carbohydrates were presented in Fig.12 (a2) and Fig.12 (b2) respectively. It was found that the pore size is about 0.33-0.42nm. From the rejection behavior, it was found that the MWCO of the result membrane is about 1000Da. In addition to these, they also have small  $\sigma$ , indicating that they have narrow pore size distributions. Two tests using different solutes all proved it a nice NF membrane in pore size, pore size distribution and MWCO.

**Table 2** Rejection of neutral solutes used during pore size distribution.

Solute	MW ( $\text{g} \cdot \text{mol}^{-1}$ )	Rejection (%)
PEG200	200	64.52 $\pm$ 4.23
PEG 400	400	90.69 $\pm$ 2.37
PEG 600	600	94.72 $\pm$ 2.07
PEG 1000	1000	97.34 $\pm$ 1.56
PEG 2000	2000	97.69 $\pm$ 2.11
Glucose	180	63.56 $\pm$ 3.72
Surcfose	342	82.79 $\pm$ 2.83
Raffinose	504	92.50 $\pm$ 1.79



**Fig.12.** (a1), (b1) cumulative pore size distribution curves and (a2), (b2) probability density function curves of the DCH-TMC/PSF NF membranes.

### 3.4.3 Anti-biofouling performance of the composite nanofiltration membranes

Biofouling caused by bacterial film formation on the surface of membrane is a severe problem during nanofiltration process<sup>52, 53</sup>. Foulants can adsorb to the membranes surface due to hydrophobic interactions, hydrogen bonding, van der Waals attraction, and electrostatic

interactions<sup>54</sup>. In this study, the effect of biofouling on the result NF membrane was evaluated by measuring the variation of water flux. It was clearly seen from Fig.13 that the flux declined notably within the first 1.5h, which was caused by concentration polarization and membrane fouling. In the sequential operation and re-suspension of BSA reached equilibrium due to the rigorous stirring near the membrane surface, so that a stable flux was obtained. At this moment, the *DR* value of SCHS/DCH-TMC composite membrane and DCH-TMC composite membrane were 12.9% and 52.5% respectively. Finally, the flux recovered to a stable high-level after simple water washing. The *FRR* value of SCHS/DCH-TMC composite membrane and DCH-TMC composite membrane reached to 98.9% and 73.7%. In the above test, the result NF membrane exhibited the excellent antifouling property, which attribute to the addition of SCHS .

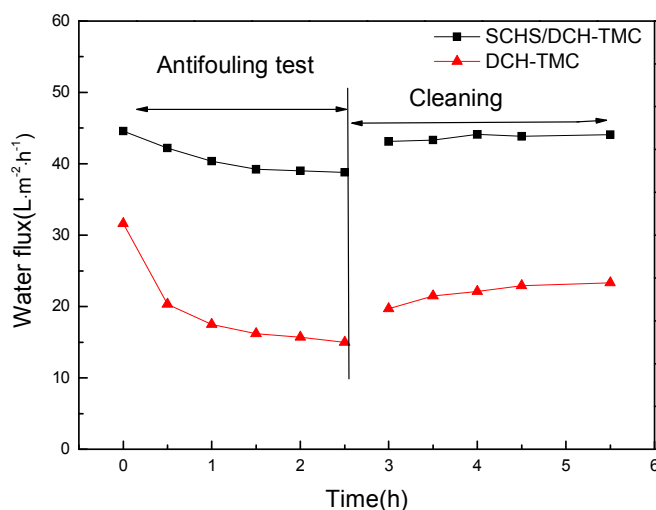


**Fig.13. Time dependent fluxes of the result NF membrane in antifouling evaluation. The filtration operation was carried out at a temperature of 25°C and operation of 0.6 MPa.**

#### 3.4.4 Dynamic water contact angle of the composite nanofiltration membranes

Dynamic water contact angle of membranes (Fig.14) demonstrates that the hydrophilicity of PSF supporting membrane was improved. This is because DCH-TMC composite membrane has many hydrophilic groups. They are carboxyl, amine and acylamino. Obviously, the hydrophilicity of SCHS /DCH-TMC composite membrane is superior. This is attributed to the hydroxyl group of SCHS. This result also indicates that the active layer successfully formed in the surface of NF membrane.

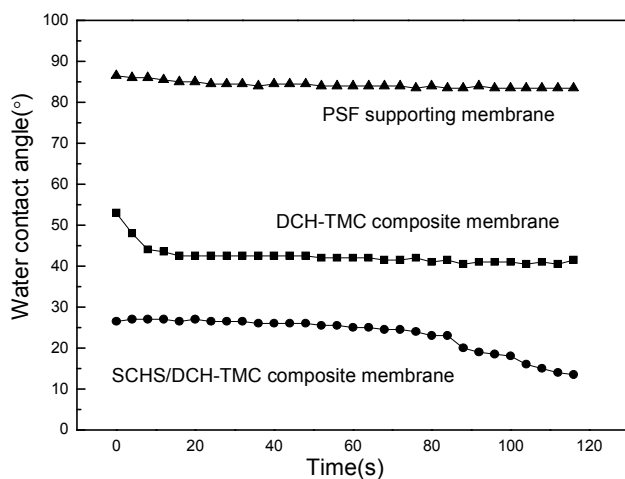


**Fig.14. Dynamic water contact angle of the membranes**

### 3.4.5 Stability of the composite nanofiltration membranes in long-time running

Long-time stability of the composite nanofiltration membrane was also very important for the practical application. The water flux and salt rejection of the result membrane during 10 days of filtration were presented in Fig.15. The results showed slight variation in water flux and rejection of  $\text{Na}_2\text{SO}_4$ , which showed the excellent stability during 10days of operation. The composite nanofiltration membrane with 0.07% (w/v) SCHS added kept a high permeation flux (approximately  $40\text{L} \cdot \text{m}^{-2}\text{h}^{-1}$  pure water flux) and identical rejection (approximately 98%  $\text{Na}_2\text{SO}_4$  rejection) during the whole testing period.

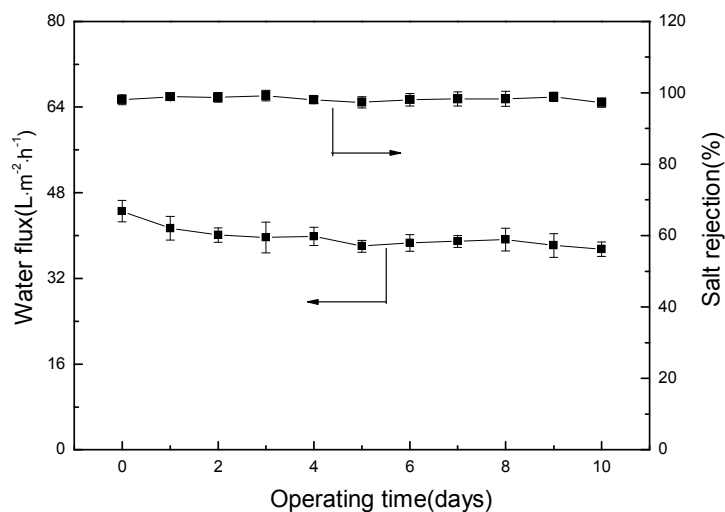


**Fig.15. Long-term testing of the result NF membrane during 10 days tested with 2000ppm Na<sub>2</sub>SO<sub>4</sub> at 0.6MPa, 25°C and PH7.0.**

#### 4. Conclusions

In this work, a simple and effective approach has been demonstrated for a novel NF membrane. Thin-film composite polyamide nanofiltration membranes were successfully prepared by interfacial polymerization technique from DCH and TMC, which was proved by ATR-FTIR and SEM images and measured by NF system (Fig.2).

The key finding is that the addition of SCHS has significant influence on the NF performance of the resultant DCH-TMC composite membrane. The result NF membrane prepared under the optimum condition exhibited Na<sub>2</sub>SO<sub>4</sub> rejection of 98.1% and the water flux of 44.6Lm<sup>-2</sup>h<sup>-1</sup> under 0.6MPa. The rejection of Na<sub>2</sub>SO<sub>4</sub>, MgSO<sub>4</sub>, MgCl<sub>2</sub> and NaCl follows a decreasing in order of 98.1%, 92.0%, 80.6 % and 27.0 % respectively. The pore size of the NF membrane is about 0.33-0.42nm and the MWCO of the NF membrane is about 1000Da which was calculated with two different methods. In addition, the NF membrane also showed the ability of anti-fouling, hydrophilic and good stability.

#### Acknowledgments

The authors are thankful for the financial support received from the National Natural Science Foundation of China (51172144), Shanghai Union Program (LM201249), the Key Technology R&D Program of Shanghai Committee of Science and Technology in China (13521102000 and

14231201503 ) , 2013 Year Special Project of the Development and Industrialization of New Materials of National Development and Reform Commission in China (20132548) and the Key Technology R&D Program of Jiangsu Committee of Science and Technology in China (BE2013031).

## References

1. N. Hilal, H. Al-Zoubi, N. A. Darwish, A. W. Mohamma and M. Abu Arabi, *Desalination*, 2004, 170, 281-308.
2. B. V. Bruggen, C. Vandecasteele, *Environmental Pollution*, 2003,122, 435-445.
3. L. Shu, T.D. Waite, P.J. Bliss, *Desalination*,2005,172,235-243
4. T. Gotoh, H. Iguchi and K.-I. Kikuchi, *Biochemical Engineering Journal*, 2004, 19, 165-170.
5. N. K. Saha and S. V. Joshi, *Journal of Membrane Science*, 2009, 342, 60-69.
6. C. Wu, S. Zhang, D. Yang and X. Jian, *Journal of Membrane Science*, 2009, 326, 429-434.
7. B. Van der Bruggen, M. Mänttari and M. Nyström, *Separation and Purification Technology*, 2008, 63, 251-263.
8. X. Li, Y. Cao, H. Yu, G. Kang, X. Jie, Z. Liu and Q. Yuan, *Journal of Membrane Science*, 2014, 466, 82-91.
9. Y. Zhang, Y. Su, J. Peng, X. Zhao, J. Liu, J. Zhao and Z. Jiang, *Journal of Membrane Science*, 2013, 429, 235-242.
10. M. Liu, Y. Zheng, S. Shuai, Q. Zhou, S. Yu and C. Gao, *Desalination*, 2012, 288, 98-107.
11. Q.-F. An, W.-D. Sun, Q. Zhao, Y.-L. Ji and C.-J. Gao, *Journal of Membrane Science*, 2013, 431, 171-179.
12. D. Hu, Z.-L. Xu and Y.-M. Wei, *Separation and Purification Technology*, 2013, 110, 31-38.
13. W. Xie, G. M. Geise, B. D. Freeman, H.-S. Lee, G. Byun and J. E. McGrath, *Journal of Membrane Science*, 2012, 403-404, 152-161.
14. D. Hu, Z.-L. Xu and C. Chen, *Desalination*, 2012, 301, 75-81.
15. T.V.Gestel, C.Vandecasteele, A.Buekenhoudt, *Journal of Membrane Science*, 2002,207,73-89
16. N. Hilal, M. Al-Abri, H. Al-Hinai and M. Abu-Arabi, *Desalination*, 2008, 221, 284-293.
17. L.-B. Zhao, Z.-L. Xu, M. Liu and Y.-M. Wei, *Journal of Membrane Science*, 2014, 454, 184-192.
18. S. Zhang, F. Fu and T.-S. Chung, *Chemical Engineering Science*, 2013, 87, 40-50.
19. Y. Cui, H. Wang, H. Wang and T.-S. Chung, *Chemical Engineering Science*, 2013, 101, 13-26.
20. S. P. Sun, T. A. Hatton, S. Y. Chan and T.-S. Chung, *Journal of Membrane Science*, 2012, 401-402, 152-162.
21. P. H. H. Duong, T.-S. Chung, K. Jeyaseelan, A. Armugam, Z. Chen, J. Yang and M. Hong, *Journal of Membrane Science*, 2012, 409-410, 34-43.
22. G. Han, S. Zhang, X. Li, N. Widjojo and T.-S. Chung, *Chemical Engineering Science*, 2012, 80, 219-231.
23. J. Xiang, Z. Xie, M. Hoang, D. Ng and K. Zhang, *Journal of Membrane Science*, 2014, 465, 34-40.
24. J. Xiang, Z.I.Xie, M.Hoang, *Journal of Membrane Science*,2014, 465,34-40.
25. Y. Li, Y. Su, Y. Dong, X. Zhao, Z. Jiang, R. Zhang and J. Zhao, *Desalination*, 2014, 333, 59-65.
26. W. Chen, Y. Su, J. Peng, Y. Dong, X. Zhao and Z. Jiang, *Advanced Functional Materials*, 2011, 21, 191-198.

27. P.-Y. Zhang, Z.-L. Xu, H. Yang, Y.-M. Wei, W.-Z. Wu and D.-G. Chen, *Desalination*, 2013, 319, 47-59.
28. B. A. Anderson, A. Literati, B. Ball and J. Kubelka, *Spectrochimica acta. Part A, Molecular and biomolecular spectroscopy*, 2015, 134, 473-483.
29. A. K. Ghosh, B.-H. Jeong, X. Huang and E. M. V. Hoek, *Journal of Membrane Science*, 2008, 311, 34-45.
30. S. A. SUNDET, W. A. MURPHEY, S. B. SPECK, *Journal of Polymer Science* 1959,XL, 389-397.
31. S. Muthu, G. Ramachandran, E. Isac Paulraj and T. Swaminathan, *Spectrochimica acta. Part A, Molecular and biomolecular spectroscopy*, 2014, 128, 603-613.
32. Y. Ji, Q. An, Q. Zhao, H. Chen and C. Gao, *Journal of Membrane Science*, 2011, 376, 254-265.
33. M. N. A. Seman, M. Khayet and N. Hilal, *Journal of Membrane Science*, 2010, 348, 109-116.
34. Y. Liu, B. He, J. Li, R. D. Sanderson, L. Li and S. Zhang, *Journal of Membrane Science*, 2011, 373, 98-106.
35. X.-Z. Wei, L.-P. Zhu, H.-Y. Deng, Y.-Y. Xu, B.-K. Zhu and Z.-M. Huang, *Journal of Membrane Science*, 2008, 323, 278-287.
36. Y.-C. Chiang, Y.-Z. Hsub, R.-C. Ruaan, C.-J. Chuang and K.-L. Tung, *Journal of Membrane Science*, 2009, 326, 19-26.
37. F. Yang, S. Zhang, D. Yang and X. Jian, *Journal of Membrane Science*, 2007, 301, 85-92.
38. S. Yu, M. Ma, J. Liu, J. Tao, M. Liu and C. Gao, *Journal of Membrane Science*, 2011, 379, 164-173.
39. R. Nadler and S. Srebnik, *Journal of Membrane Science*, 2008, 315, 100-105.
40. S. S. Dhumal and A. K. Suresh, *Polymer*, 2009, 50, 5851-5864.
41. W.Xie, G.M. Geise, B.D. Freeman, *Journal of Membrane Science*, 2012,403, 152-161.
42. D.Hu, Z.-L.Xu, C. Chen, *Desalination* 2012, 301, 75-81.
43. A. Ahmad and B. Ooi, *Journal of Membrane Science*, 2005, 255, 67-77.
44. B. Su, T. Wang, Z. Wang, X. Gao and C. Gao, *Journal of Membrane Science*, 2012, 423-424, 324-331.
45. A. Abidi, N. Gherraf, S. Ladjel, M. Rabiller-Baudry and T. Bouchami, *Arabian Journal of Chemistry*, 2011.
46. P. Daraei, S. S. Madaeni, N. Ghaemi, H. Ahmadi Monfared and M. A. Khadivi, *Separation and Purification Technology*, 2013, 104, 32-44.
47. J.M.M. Peeters, J.P. Boom, M.H.V. Mulder, *Journal of Membrane Science*, 1998, 145, 199-209.
48. X.-X. Xu, C. -L.Zhou, B.-R.Zeng, H.-P.Xia, W.-G.Lan and X.-M.He, *Separation and Purification*, 2012, 96, 229-236
49. Y.Li, Y.Su, J.Li, X.Zhao, X.Fan, J.Zhu, Y.Ma, Y.Liu and Z.Jiang, *Journal of Membrane Science*, 2015, 476, 10-19.
50. B.B.Tang, Z.B.Huo, P.Y.Wu, *Journal of Membrane Science*, 2008, 320, 198-205.
51. H.W.Sun, G.H.Chen, R.H.Huang, C.J.Gao, *Journal of Membrane Science*, 2007, 297, 51 - 58.
52. Y.-C. Chiang, Y. Chang, C.-J. Chuang and R.-C. Ruaan, *Journal of Membrane Science*, 2012, 389, 76-82.
53. Y.-L. Ji, Q.-F. An, Q. Zhao, W.-D. Sun, K.-R. Lee, H.-L. Chen and C.-J. Gao, *Journal of Membrane Science*, 2012, 390-391, 243-253.
54. Y.-N. Wang and C. Y. Tang, *Journal of Membrane Science*, 2011, 376, 275-282.